

**SINGLE PARTICLE DIFFRACTION AT FLASH\***

M. Bogan<sup>#</sup>, S. Boutet, Dmitri Starodub, Philippe Decorwin-Martin, SLAC National Accelerator Laboratory, Menlo Park, CA, 94025 U.S.A.

H. Chapman, S. Bajt, J. Schulz, Centre for Free-Electron Laser Science, DESY, Hamburg, Germany

Janos Hajdu, M. M. Seibert, Bianca Iwan, Nicusor Timneanu, Laboratory of Molecular Biophysics, Department of Cell and Molecular Biology, Uppsala University, Uppsala, Sweden

Stefano Marchesini, Lawrence Berkeley National Laboratory, Berkeley, CA 94720, USA

Anton Barty, W. Henry Benner, Matthias Frank, Stefan P. Hau-Riege, Bruce Woods, Lawrence Livermore National Laboratory, Livermore CA 94550, USA

Urs Rohner, TOFWERK AG, Thun, Switzerland

*Abstract*

Single-pulse coherent diffraction patterns have been collected from randomly injected single particles with a soft X-ray free-electron laser (FEL).[1] The intense focused FEL pulse gives a high-resolution low-noise coherent diffraction pattern of the object before that object turns into a plasma and explodes. A diffraction pattern of a single particle will only be recorded when the particle arrival into the FEL interaction region coincides with FEL pulse arrival and detector integration. The properties of the experimental apparatus coinciding with these three events set the data acquisition rate. For our single particle FLASH diffraction imaging experiments: (1) an aerodynamic lens stack prepared a particle beam that consisted of particles moving at 150-200 m/s positioned randomly in space and time, (2) the 10 fs long FEL pulses were delivered at a fixed rate, and (3) the detector was set to integrate and readout once every two seconds. The effect of these experimental parameters on the rate of data acquisition using randomly injected particles will be discussed. Overall, the ultrashort FEL pulses do not set the limit of the data acquisition, more important is the effective interaction time of the particle crossing the FEL focus, the pulse sequence structure and the detector readout rate. Example diffraction patterns of randomly injected ellipsoidal iron oxide nanoparticles in different orientations are presented. This is the first single particle diffraction data set of identical particles in different orientations collected on a shot-to-shot basis. This data set will be used to test algorithms for recovering 3D structure from single particle diffraction.

\*This work was supported by the following agencies: The U.S. Department of Energy by Lawrence Livermore National Laboratory in part under Contract W-7405-Eng-48 and in part under Contract DE-AC52-07NA27344, Lawrence Livermore National Laboratory (the project 05-SI-003 from the Laboratory Directed Research and Development Program of LLNL); the U.S. Department of Energy by the SLAC National Accelerator Laboratory in part under contract number DE-AC02-76SF00515; the Deutsches Elektronen-Synchrotron, a research center of the Helmholtz Association. Additional support comes from the DFG Cluster of Excellence at the Munich Centre for Advanced Photonics ([www.munich-photonics.de](http://www.munich-photonics.de)), from the Virtual Institute Program of the Helmholtz Society, and by the Swedish Research Council.

<sup>#</sup>mbogan@slac.stanford.edu

**INTRODUCTION**

A new era of research with hard X-ray FELs will soon be initiated when the Linac Coherent Light Source (LCLS) at the SLAC National Accelerator Laboratory initiates user operations in the fall of 2009. The FLASH soft X-ray free-electron-laser (FEL) in Hamburg[2] has provided opportunities for testing ultrafast imaging of single particles using “diffract and destroy” experiments[3, 4] proposed to solve non-periodic biological structure at LCLS.[5] Highlights of our FLASH diffraction imaging experiments will be reviewed briefly here. FLASH operating at 32 and 13.5 nm was used to generate single pulse coherent diffraction patterns from nanostructured nonperiodic objects.[1, 6-9] Iterative phase retrieval algorithms are used to reconstruct images of the objects from the diffraction patterns.[10] Extending this approach with the <1 nm wavelength pulses from hard-X-ray FELs is anticipated to eventually facilitate atomic resolution imaging of nanometer-to-micrometer-sized objects without the need for crystallization.[3, 5, 11]

Chapman *et al.*'s femtosecond diffractive imaging experiment proved that diffraction-limited resolution images could be obtained from the exposure of nanostructured non-periodic objects to single FLASH pulses.[9] The key to recording the diffraction patterns is a specially designed camera consisting of a laterally graded multilayer mirror that reflects the diffraction pattern onto a CCD camera and allows the intense FEL pulse to pass through a hole.[12] The mirror also acts as a bandpass filter for both wavelength and angle.

The long wavelengths produced by FLASH (7-32 nm) require the development of sample handling capabilities tuned for larger objects (50 nm to 3  $\mu$ m). This size range is well covered by many different types of commercially available spherical size-monodisperse standards, such as polymer-based spheres commonly used in biomedical diagnostics, chromatography, and aerosol science. These spheres have played a key role in the development of coherent X-ray diffractive imaging experiments at FLASH. A continuum model for the imaging experiments performed at FLASH[13] and femtosecond time-resolved measurements of nanoscale dynamics[8] show that

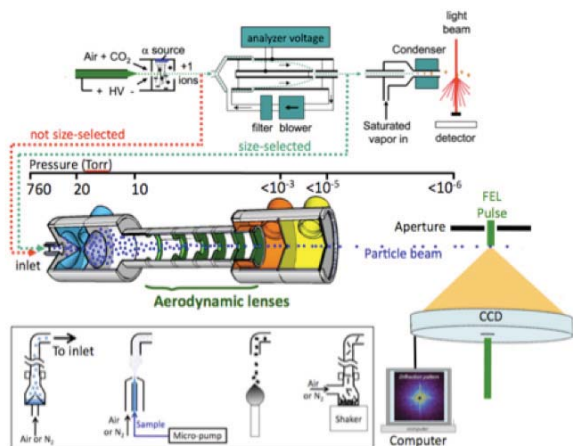


Figure 1: Conceptual schematic of single-pulse X-ray scattering from single particles in a substrate-free manner. (A) In one variation, electro sprayed spherical nanoparticles are size-selected by differential mobility analysis prior to introduction to the differentially-pumped aerodynamic lens stack. The particle beam is steered into the FEL and single pulse diffraction patterns are recorded on a CCD. Alternative aerosol sources we have tested include nebulizers, atomizers, flames, and dispersion of dry powders.

irradiated 140 nm diameter spheres maintain their integrity during the 25 fs pulses. These measurements were facilitated by the size-monodispersity of the spheres, which was enhanced by a differential mobility method.[14] The results gave credence to the concept of imaging individual nanometer and sub-nanometer-sized objects such as single molecules or larger clusters of molecules using hard X-ray FELs in the future. The first experimental evidence of single particle FLASH diffraction imaging shortly followed. Image reconstruction of individual 145 nm diameter spheres supported by a 20 nm thick silicon nitride membrane was performed with the aid of a strong-scattering reference.[6] Two of the factors that motivate use of sample handling systems free of supporting membranes include, (1) adequate oversampling necessitates an isolated sample and (2) elimination of spurious signal contributions due to substrate scattering.

Aerodynamically focused particle beams are being specifically developed for introducing aerosols, nanoparticles, viruses, cells and biomolecules into the X-ray beam[1] (Fig. 1). Based on work by Liu *et al.*, the apparatus implements thin plate orifices to manipulate the particle spatial distribution prior to them passing through a nozzle and subsequently undergoing supersonic expansion into vacuum.[15, 16] An axisymmetric stack of these thin plate orifices, or aerodynamic lenses, provides successive contractions of a flowing particle beam cross section and enables focusing of a wide range of particle sizes (1 nm to 10  $\mu\text{m}$ ).[17]

The inlet of the aerodynamic lens stack samples aerosolized particles from atmospheric pressure at a rate

of 0.86 liters per minute and injects them into a vacuum chamber to meet a FEL pulse. Any method that generates aerosol at atmospheric pressure can be coupled to the aerodynamic lens stack.

Polystyrene spheres were used to help determine differential pumping pressures to optimize focusing of particle sizes over the range of 70 nm to 2  $\mu\text{m}$  and as standards for measuring particle injection rate into vacuum. Single particle charge detection was used to visualize and align particle beams of electro sprayed spheres in vacuum relative to the laser pulses.[14, 18]

Here we provide a general discussion of capturing single particle diffraction from randomly injected particles at FLASH and report capture of single-shot diffraction patterns of ellipsoidal iron oxide nanoparticles in random orientations.

### *On Collecting FLASH Diffraction of Randomly Injected Particles in Flight*

Consider a particle beam randomly injected through an aerodynamic lens perpendicular to a pulsed laser. The most common type of this experiment is single particle aerosol mass spectrometry (SPAMS).[19] The effective time a particle is present in the interaction region, or effective interaction time, is set primarily by the particle's velocity and the diameter of the focus of the laser. The relatively large laser diameter in SPAMS experiments sets the interaction time for a particle moving at 200 m/s to a couple of microseconds. This time is long relative to the typically 3 ns pulsed laser used for desorption/ionization. In SPAMS the data is recorded as a mass spectrum, timed to readout out after each laser pulse is fired.

Collecting diffraction patterns of single particles in flight using ultrafast X-ray lasers has some similarities to aerosol mass spectrometry experiments and relies on the coincidence of three events: (1) particle presence in the interaction region, (2) FEL pulse in the interaction region, and (3) CCD data acquisition during a coincidence of (1) & (2). Figure 3 shows the effective interaction time for

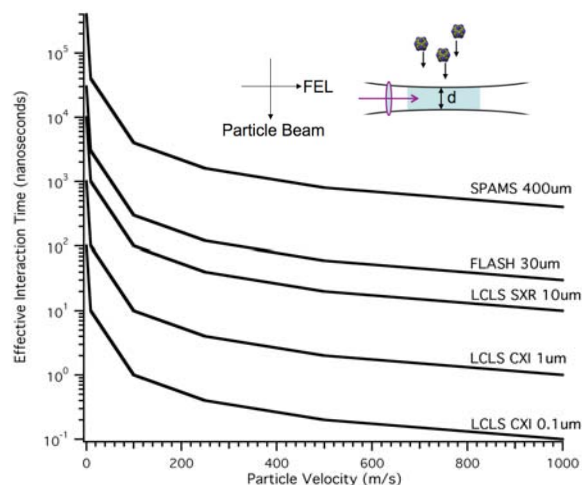


Figure 2: Estimated effective interaction time, in a perpendicular geometry, for a particle passing through different interaction regions with diameter,  $d$ , as a function of velocity.

Table 1: X-ray FEL pulse parameters and relative particle hit rates for randomly injected particles assuming maximum pulse rate delivery and identical focus for each source

FEL	Pulse separation	Max pulses per bunch	Max pulses/sec	Relative hit rate
FLASH	1, 10 $\mu$ s	800	4000	1
LCLS	8.3 ms	1	120	0.03
Euro XFEL	200 ns	3000	30000	7.5

several single particle laser interaction experiments in a perpendicular geometry. The FLASH diameter of 30  $\mu$ m at the interaction region gives an interaction time in the range of hundreds of nanoseconds for a particle moving at 200 m/s. In this case the effective interaction time is many orders of magnitude longer than the ultrafast FEL pulses, typically <20 fs from FLASH.

The effective interaction time is an important parameter to consider when planning single particle diffraction experiments with randomly injected particles at various FELs because it can dramatically impact data acquisition rates. Table 1 shows the pulse sequence parameters at FLASH and those anticipated for LCLS and the Euro XFEL. For example, consider a randomly injected particle beam moving at 150 m/s into FLASH operating in microbunch mode with 1  $\mu$ s pulse separation, a 30  $\mu$ m focus and the maximum pulses per bunch. Over the 800  $\mu$ s of a single microbunch, the particle would see FEL in the interaction region for 200 ns x 800 pulses = 160  $\mu$ s or 20 % of the time during the microbunch delivery. FLASH microbunches are delivered 5 times per second so a total of 800  $\mu$ s of FEL each second is available to interact with the randomly injected particles. This is much longer than the 80 ps total time of the FEL pulses.

The hard X-rays from the LCLS are designed to have an even tighter focus, from 10  $\mu$ m at first operation down to 100 nm required to perform single molecule imaging on the Coherent X-ray Imaging (CXI) apparatus. For CXI, a molecule moving 150 m/s would be in the interaction region for less than 1 ns. Schemes to control particle velocity or time particle injection must account for the effective FEL pulse dimensions at the interaction region. The following section will provide an example of typical diffraction pattern data acquisition from single nanoparticles at FLASH.

### Single Particle Diffraction of Ellipsoidal Nanoparticles

Figure 2 shows a scanning electron microscope image of the test sample, ellipsoidal iron oxide nanoparticles (Corpuscular, NY). Aerosols of these particles were generated by two methods. In an atomizer, a gas is used to aspirate the liquid into a (usually) sonic velocity gas jet, wherein it is sheared into droplets. In a nebulizer, this liquid/gas is impacted against a barrier to remove the larger fraction of the droplets. Disposable nebulizers

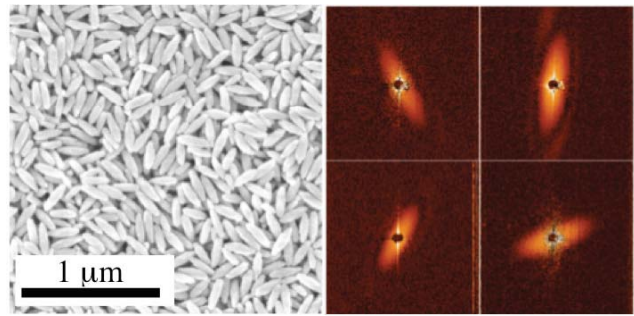


Figure 3: Scanning electron micrograph of ellipsoidal 50 nm x 250 nm iron oxide nanoparticles. Diffraction patterns of single particles in different orientations collected at FLASH, 7 nm, 10 fs, 10<sup>12</sup> ph/pulse.

(Salter Labs, Arvin, CA) were used to aerosolize 2-5 ml of solutions containing nanoparticles with a stream of nitrogen gas (flow rate of 1.0-2.5 L/min).

The camera[12] had a laterally graded multilayer mirror, which reflected the diffraction pattern onto a CCD detector at a distance of 54.9 mm from the specimen. The mirror worked as a bandpass filter for both wavelength and scattering angle, and isolated the desired scattering pattern from incoherent and plasma emission arising from the sample, and from non-sample-related scattering. A hole in the centre of the mirror allowed the direct beam to pass harmlessly through the instrument into a beam dump at a distance behind the instrument.

Figure 4 shows an example of the diffraction pattern acquisition rate for randomly injected ellipsoidal nanoparticles for this scenario. FLASH was operating with 100 pulses per bunch or 500 pulses per second total. This diffraction pattern acquisition rate is typical for our apparatus with nebulized nanoparticle solutions of about 10<sup>12</sup> particles/ml.

A critical parameter in the data acquisition sequence is the detector readout rate. For the data in Fig. 4, the detector integration and readout time were equal, one second for each. Recall that a diffraction pattern of a single particle will only be recorded when the particle arrival into the FEL interaction region coincides with FEL pulse arrival and detector integration. Thus, 50 % of the random particle arrival and FEL overlaps were not

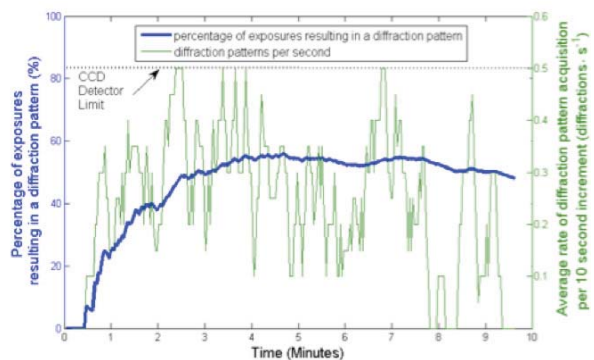


Figure 4: Instantaneous and average diffraction pattern acquisition rate for nebulized ellipsoidal nanoparticles.

recorded and the data acquisition rate was limited to 0.5 patterns/second. Since data acquisition from random injection follows Poisson statistics, the actual particle/FEL coincidence rate is  $>1$  per second when diffraction patterns are recorded with subsequent readouts. To access all of this potential data, faster detectors are being developed. The 0.5 patterns per second rate is an order of magnitude larger than achieved previously. Developments in particle tracking, triggered particle sources, and triggered XFEL sources will also continue to increase the efficiency of data acquisition.

The ellipsoidal nanoparticles were chosen because they are an ideal test sample to investigate relative orientation of individual particles at the interaction region. These particles strongly scatter and their diffraction patterns are clearly indicative of their orientation. At the instant the X-ray pulse interacts with the particle, a snapshot of the particle's orientation is encoded in the diffraction pattern. Diffraction patterns from 4 individual particles are shown in Fig. 2. This type of data set has been proposed to be used for determining three-dimensional structures of identical particles using iterative phase retrieval.[3]

To use iterative phase retrieval to recover the 3D structure, particle orientation must be determined for each diffraction pattern. One approach is the use of spatial correlation analysis of scattered intensity fluctuations applied to the complete data set of all diffraction patterns in order to recover a 3D diffraction volume. This method was first developed for solution scattering from many particles[20], and recently adopted to a single-molecule XFEL diffraction experiment.[21] While a simple sum of individual diffraction patterns results in a spherically averaged image, producing the same type of data as in the small angle X-ray scattering (SAXS), averaging of the *products* of scattered intensities in different pixels enhances the scattering from the single particle, thus revealing information additional to the SAXS data. The major challenge in this method is calculation of the coefficients  $S_{lm}(k)$  in the spherical harmonics expansion of scattered intensity  $S(\mathbf{k})$  from the equation  $C_l(k_1 k_2) = \sum_m S_{lm}(k_1) S_{lm}^*(k_2)$ , where  $C_l(k_1 k_2)$  is an  $N \times N$  matrix, directly obtained from the experimental data binned to a grid of  $N$  scattering vector absolute values. The special solutions for  $S_{lm}(k)$  can be easily obtained, but since equations for different  $l$  are independent, a special effort is required to relate the coefficients corresponding to different values of  $l$ . In principle, this can be done by involving higher order correlations.[22] The situation is greatly simplified in the case of ellipsoidal iron oxide nanoparticles, which possess an axis of rotation. If this axis is aligned with the  $z$ -axis, then only coefficients with  $m \neq 0$  will have non-zero values. When all coefficients  $S_{lm}(k)$  up to a required resolution are determined, the 3-dimensional distribution of scattered intensity is known as well. Subsequently, iterative phase retrieval algorithms[10] can be applied to reconstruct the object electron density. Application of the

spatial correlation approach to the single particle diffraction using ultra-fast X-ray pulses reduces experimental difficulties associated with implementation of this method to solution scattering using traditional X-ray sources. First, it eliminates the background of solvent and spherically averaged particle scattering, inevitable in solution scattering. Second, as the right panel of Fig. 3 clearly demonstrates, a single pulse provides more than adequate scattered intensity from a 'frozen' particle. In contrast, in solution scattering it can be problematic to choose the exposure time, long enough to achieve several scattering events from the same particle, and short enough for particles to rotate only a small angle determined by required resolution.

## CONCLUSION

We have collected the first single-shot X-ray diffraction data set that mimics the kind of "diffract and destroy" data required to obtain 3D structure of injected particles from XFELs. We will use this test data set to develop robust algorithms for determining particle orientations and 3D structure.

## REFERENCES

- [1] M. J. Bogan *et al.*, Nano. Lett. **8**, 310 (2008).
- [2] W. Ackermann *et al.*, Nat. Photonics **1**, 336 (2007).
- [3] G. Huldt, A. Szoke, and J. Hajdu, J. Struct. Biol. **144**, 219 (2003).
- [4] K. E. Schmidt *et al.*, Phys. Rev. Lett. **101**, 115507 (2008).
- [5] R. Neutze *et al.*, Nature **406**, 752 (2000).
- [6] S. Boutet *et al.*, J. Elec. Spectros. Rel. Phenom. **166-167**, 65 (2008).
- [7] A. Barty *et al.*, Nat. Photonics **2**, 415 (2008).
- [8] H. N. Chapman *et al.*, Nature **448**, 676 (2007).
- [9] H. N. Chapman *et al.*, Nat. Physics **2**, 839 (2006).
- [10] S. Marchesini, Rev. Sci. Inst. **78**, 011301 (2007).
- [11] J. C. H. Spence, and B. Doak, Phys. Rev. Lett. **92**, 198102 (2004).
- [12] S. Bajt *et al.*, Appl. Opt. **47**, 1673 (2008).
- [13] S. P. Hau-Riege *et al.*, Phys Rev E **76**, 046403 (2007).
- [14] M. J. Bogan *et al.*, J. Aerosol Sci. **38**, 1119 (2007).
- [15] P. Liu *et al.*, Aerosol Sci. Tech. **22**, 314 (1995).
- [16] P. Liu *et al.*, Aerosol Sci. Tech. **22**, 293 (1995).
- [17] A. S. Wexler, and M. V. Johnston, *Real-time single-particle analysis* (John Wiley & Sons, Hoboken, New Jersey, 2005), pp. 365.
- [18] W. H. Benner *et al.*, J. Aerosol Sci. **39**, 917 (2008).
- [19] M. J. Bogan *et al.*, Rapid Communications in Mass Spectrometry **21**, 1214 (2007).
- [20] Z. Kam, Macromolecules **10**, 927 (1977).
- [21] D. K. Saldin *et al.*, J. Phys.: Condens. Matter **21**, 134014 (2009).
- [22] Z. Kam, J. Theor. Biol. **82**, 15 (1980).